1 Manufacture of Fillers

The history of particulate fillers used in rubber is almost as long as that of rubber itself[1–3]. One aspect of filler addition has been improvement of rubber properties. Another aspect was extension of the rubber with less expensive materials. After Hancock developed the earliest device using rollers to crumb natural rubber (NR) in 1820, and the two-roll mill for NR mastication and compounding was patented by Chaffee in 1836 and 1841, incorporation of inert fillers in finely divided particulate form became standard practice. Fillers such as ground limestone, barites, clay, kaolin, etc. were used in order to extend and cheapen the compounds since it was found that in natural rubber, quite a bit of filler could be added without detracting too much from the final vulcanizate properties. Zinc oxide was originally used for its whiteness, and later was found to have some reinforcing effect, becoming known as an "active" filler. Carbon black, which was known as a black pigment, was also found to be able to improve the rubber properties significantly at low concentrations, especially the stiffness. Systematic studies of the effect of fillers had been reported by Heinzerling and Pahl in Germany in 1891. Part of this effect may be due to its activating effect on many vulcanization accelerators for which zinc oxide is still utilized. In 1904, Mote in England, discovered the reinforcing effect of carbon black. He reported that the tensile strength of the filled NR increased drastically, compared with the values obtained with the techniques of that time. Although automobiles had been around and running on rubber tires for more than a decade, the importance of this discovery was recognized and developed when black tires were demonstrated to have better wear resistance than white ones, which contained mainly zinc oxide as a filler. Carbon black is now the most important filler used in rubber. In the last century, the production techniques and designation of types of carbon black have developed rapidly.

In the meantime, non-black fillers have also developed. Among these non-black ones, the first reinforcing filler, calcium silicate, was introduced in 1939. It was prepared by wet precipitation from sodium silicate solution with calcium chloride. In further development of the process, the calcium was leached out by hydrochloric acid to yield a reinforcing silica pigment of comparable particle size. About 10 years later, direct precipitation of silica from sodium silicate solution had developed to a commercial process and this is still a major process today. In 1950, a different type of anhydrous silica appeared, which was made by reacting silicon tetrachloride or silica chloroform

(trichlorosilane) with water vapor in a hydrogen-oxygen flame. Because of the high temperature at the formation (about 1400°C), this pyrogenic silica has a lower concentration of silanol groups on the surface than the precipitated silicas. The latter contain about 88%−92% SiO_2 and have ignition losses of 10%−14%, whereas pyrogenic silica contains 99.8% silica. Because of its lower surface concentration of silanols, ultra-high purity with total impurities in many cases below 100 ppm (parts per million), and much higher price, pyrogenic silica is mainly used as a filler for high cost compounds such as silicone rubber.

In contrast, since the beginning of the industrial-scale production of fine-particle silicas and silicates in 1948, precipitated silica manufacturers have always desired to find their products used in tires as well. Whereas silicas were rapidly able to replace up to 100 percent of carbon black in shoe sole materials and also made their way into the mechanical goods sector, mostly as blends with carbon blacks, their use in tires in any quantities worth mentioning has long been limited to two types of compounds: off-the-road tread compounds containing 10 phr to 15 phr of silica blended with carbon black in order to improve tear properties, and textile and steel cord bonding compounds containing 15 phr of silica, again blended with carbon black, in combination with resorcinol/formaldehyde systems[4].

During the two oil crises in the 1970s, which had led to a steep rise in the price of carbon black, the question arose whether silica in tires could be an alternative to carbon black. When the price of oil fell and the fear of a lack of availability of carbon blacks subsided, this question was soon forgotten, especially since the price of silica was always higher than that of carbon black, at least in Japan and the USA. Experience has shown that silicas only have a chance to be used in tires if they offer technological advantages which are superior to those of carbon blacks.

Two developments have created a new opportunity for silicas to be used in tires: the increased awareness of the pollution from industry and the necessity of protecting the environment have given rise to a call for tires combining a long service life with driving safety and low fuel consumption. The introduction of bifunctional organosilanes as coupling agents now permits the reinforcing mechanism of silicas to be controlled by chemical means[4,5]. Based on systematic studies of surface characteristics, polymer-filler interactions, and better understanding of compounding and processing, silica was successfully used to replace carbon black as the principal filler in the tread compound of the “green tire” patented in 1992[6]. Since then, the application of precipitated silica in tire has been continuously growing, not only in tread compounds, but also in other parts of tires.

In the last two decades, research on rubber reinforcement with particulate fillers and the development of new fillers have been very hot. Since the main fillers used in the rubber industry are still carbon blacks and silicas, the topics of this book will focus on these two materials and their derivatives.

1.1 Manufacture of Carbon Black

The history of carbon black manufacture is very long, such as in China, about 3000 B.C., carbon black for pigment use was made by burning vegetable oils in small lamps and collecting the carbon on a ceramic lid; in Egypt, carbon black was used as a pigment for paints and lacquers. Starting in 1870, natural gas began to be used as the feedstock for carbon black manufacture. Over a couple of decades, the channel process was developed in which small gas flames burning in restricted air supply impinged on iron channels. In 1976, the last channel black plant was closed in the USA, due to the pollution of smoke plumes.

A critical event in the development of the carbon black industry was the discovery of the benefits of carbon black as a reinforcing agent for rubber in 1904[1]. As the automobile became ubiquitous during the 1920s, the application of pneumatic tires grew rapidly and soon by-passed other applications, causing rapid growth in consumption of carbon black. Also in the 1920s, two other processes concerning carbon black production were introduced, both using natural gas as feedstock, but having better yields and lower emissions than the channel process. One was the thermal black process, in which a brick checker is employed and works alternately by absorbing heat from a natural gas air flame, and then giving up heat to crack natural gas to carbon and hydrogen. The other process was the gas furnace process, which is no longer practiced.

The oil furnace process was first introduced by Phillips Petroleum at its plant in Borger, Texas, in 1943. This process rapidly replaced all others for the production of carbon black for use in rubber. In a modern version of the oil furnace process, carbon black yields range from 65% downward depending on the surface area of the product. Product recovery is essentially 100% as a result of high efficiency bag filters. The overwhelming majority of carbon black reactors today are based on the oil furnace process.

1.1.1 Mechanisms of Carbon Black Formation

The formation of particulate carbon involves either pyrolysis or incomplete combustion of hydrocarbon materials. Enormous literature has been published to describe the mechanism of carbon black formation, from a series of lectures by Michael Faraday at the Royal Institution in London in the 1840s[2], to a more recent intensive review[7]. Since Faraday's time, many theories have been proposed to account for carbon formation, but controversy still exists regarding the mechanism.

Mechanisms of carbon black formation must account for the experimental observations of the unique morphology and microstructure of carbon black. These include the presence of nodules, or particles, multiple growth centers within some nodules, the fusion of nodules into large aggregates, and the paracrystalline or concentric layer

plane structure of the aggregates. It is generally accepted that the mechanism of formation involves a series of stages as follows:

Formation of gaseous carbon black precursors at high temperature – This involves dehydrogenation of primary hydrocarbon molecular species to atomic carbon or primary free radical and ions which condense to semi-solid carbon precursors (or poly-nuclear-aromatic sheet) and/or formation of large hydrocarbon molecules by polymerization which then is dehydrogenated to particle precursors[3]. Taking production of furnace black with high aromatic feedstock as an example, Figure 1.1 represents several of the possible paths that feedstock can take as it is mixed with the primary fire in the reactor at the early stage. The primary fire has excess oxygen, carbon dioxide, and water, all of which act as combustion (or oxidation) reactants to the feedstock molecules. These molecules can react with and break up any feedstock molecules into small combustion species; any feedstock that goes this route is lost for carbon black production. As there is a limit to oxidative species, the remaining feedstock can either be broken down by pyrolysis or survive and become directly involved in carbon black formation reactions. Typical pyrolysis species are hydrogen, acetylene, and polyynes, which are essentially chained acetylenes. At least two formation paths are thought to occur. The first one is ring growth from acetylene, polyyne,or polycyclic aromatic hydrocarbon (PAH) collision with PAH molecules. When the number of rings reaches five or six, the molecules become thermally stable and will only be attacked by remaining oxidant molecules. These PAH molecules will

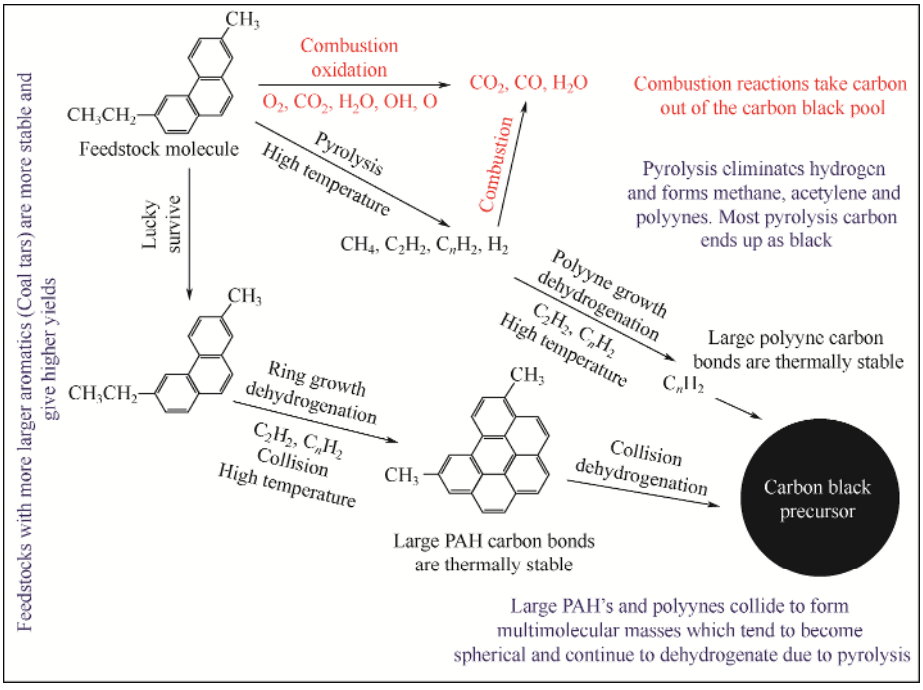

Figure 1.1 Formation of gaseous carbon black precursors

to hydrolysis. The concept of using phenolic groups as points of attachment for conventional silane treating agents has been described in several patents with the particular aim of attaching polysulfide moieties that can be vulcanized into elastomer networks for hysteresis reduction[21]. Some patents have been issued on using the acidic sites on carbon black surfaces as points of reaction of amines. In the particular case in point, the attachment was used to improve compound stability and dispersion in conductive plastics applications[22].

1.1.2.7.3 Metal Oxide Treatment

The carbon black industry has worked on ways to respond to the challenge of silica in tire treads for low rolling resistance (replacing all or some of the carbon black). Cabot has filed on, and widely published, a class of dual phase fillers in which silica or other metal oxides and carbon are co-formed in a carbon black like reactor[23–26]. In the particular product they describe, the carbon black and silica are intimately intermixed on a scale that is about the same size as the carbon black crystallite. In more recent variants, materials where the silica location is more on the exterior of the particle are described[27]. In these materials, the silica is the minor constituent. The main characteristics of these carbon blacks are their lower filler-filler interactions. Filler-polymer interactions are also increased, but by incorporating coupling agents these interactions can be adjusted as required. These materials are used as fillers for low rolling resistance, higher wet skid resistance, and improved wear resistance in tire treads when used with conventional sulfide-silane coupling agents[28,29], or as fillers for silicone rubber when used with alkyl silane and vinyl silane agents[30]. The patent literature suggests that other applications have been considered as well[31]. Patents have also been issued on coated carbon black made by depositing silica on the black surface in an aqueous solution of sodium silicate by adjusting pH with acid[32–34].

■ 1.2 Manufacture of Silica

There are two families of silicas: natural and synthetic. The former are generally crystallized, such as quartz or diatoms. They have contorted and large particles, even after milling, and do not find their application in rubber industry. By synthesis, it is possible to obtain better-defined particles in shape and especially of submicron size. There are two synthetic processes: pyrohydrolysis and precipitation. Both processes produce amorphous products. The first is performed in a high temperature vapor phase from silicon compounds, principally silicon tetrachloride, air, and hydrogen. The products are called “anhydrous” or fumed silica. They have less than 1.5% each of bound water and adsorbed water, which is defined as volatiles removed at, respectively, 105°C and in vacuum. With the precipitation process, the silicas, prepared by precipitation from water-soluble silicates, have approximately 5% each of bound and adsorbed water.

1.2.1 Mechanisms of Precipitated Silica Formation

The formation of precipitated silica is governed by a complex process in which the soluble silicic species which are present in the solution polymerize and form nuclei which grow to form spherical particles of various sizes, depending on the precipitation conditions, mainly temperature and concentration (Figure 1.6).

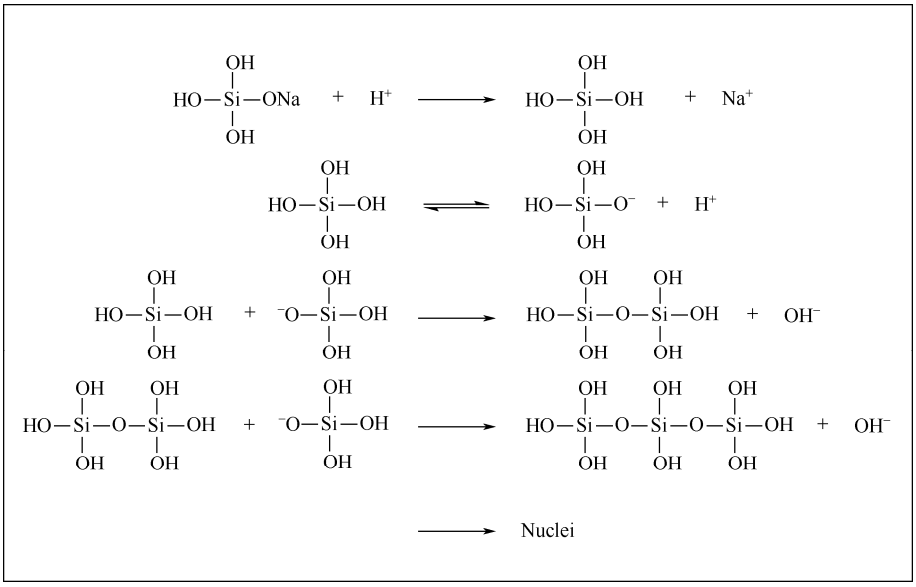

Figure 1.6 Polymerization of silicate

The polymerization, which leads to the formation and the coagulation of colloids, produces silica aggregates. Depending on the reaction conditions, the particles collide with each other forming a gel or aggregates which are then consolidated by further deposition of SiO_2 on their surface as shown in Figure 1.7[35]. Under basic pH conditions, the colloidal particles are negatively charged. They repel each other in an electrostatic way. The electrostatic repulsions are suppressed under the action of an electrolyte such as sodium cation, resulting in the coagulation of the colloidal species. The floc formed is a relatively fragile structure. An addition of water regenerates the colloids. The floc can be made rigid by polymerization of soluble silica on its surface. This is how the silica aggregates are obtained. The morphological characteristics of silica, namely its primary particle size and surface area, determine the shape and size of its aggregates and their distribution. The most important parameters governing the silica morphologies include the proportion of SiO_2 in the alkaline silicate solution, the concentration of the soluble alkali metal salt (such as sodium chloride) in the silicate solution, the reaction temperature, the speed of addition of the acid to the solution, and the other components found in the acid used[36].

2 Characterization of Fillers

Fillers are characterized by their chemical composition, micro-structure, morphology, and physical chemistry of the surface. Figure 2.1 and Figure 2.2 schematically show the basic structures of carbon black and synthetic silica, respectively. The primary dispersible unit of fillers is referred to as an "aggregate", that is, a discrete, rigid colloidal entity. It is the functional unit in well-dispersed systems. For most carbon blacks and synthetic silicas, the aggregate is composed of spheres that are fused together. These spheres are generally termed as primary "particles" or "nodules". While primary particles of silicas are composed of amorphous silicon dioxide, in carbon black aggregates, these nodules are composed of many tiny graphite-like stacks. Within the nodule of carbon blacks, the stacks are oriented so that their *c*-axis is normal to the sphere surface, at least near the nodule surface.

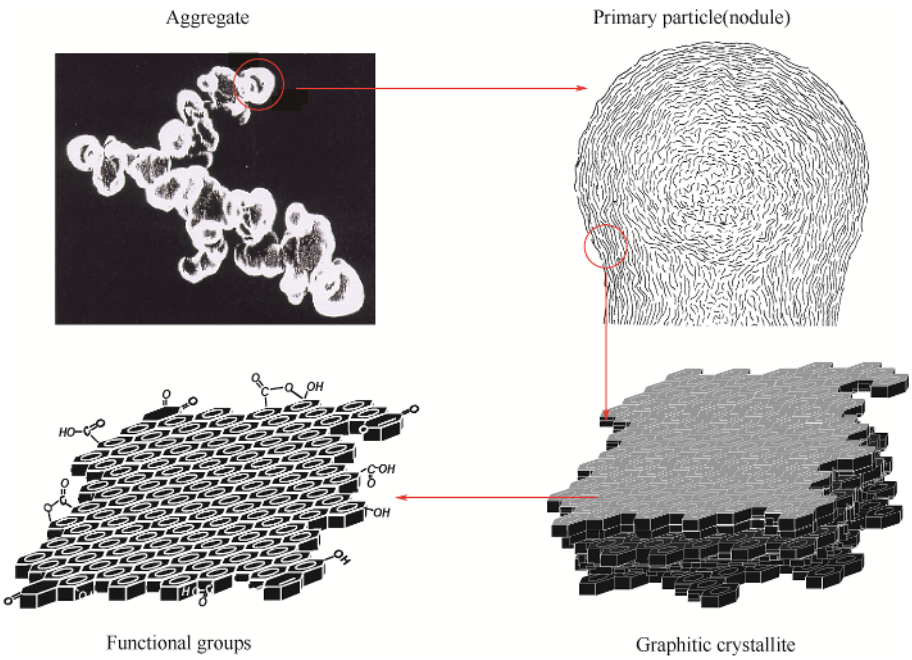

Figure 2.1 Structure of carbon black

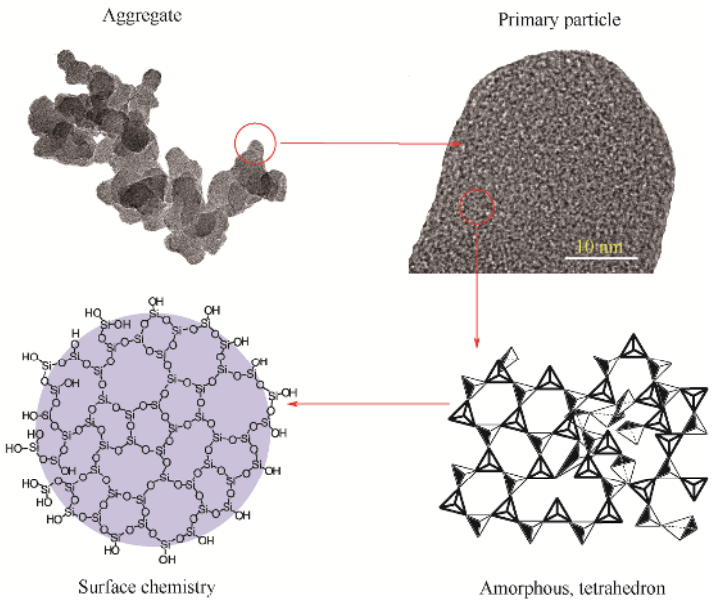

Figure 2.2 Structure of silica

■ 2.1 Chemical Composition

2.1.1 Carbon Black

Oil-furnace blacks used by the rubber industry contain over 97% elemental carbon. Thermal and acetylene blacks consist of over 99% carbon. Table 2.1 shows the chemical composition of some carbon blacks. Other elements included in furnace black, apart from carbon, are hydrogen, oxygen, sulfur, and nitrogen. In addition, there are mineral oxides, salts, and traces of adsorbed hydrocarbons. Hydrogen and sulfur are distributed on the surface and the interior of the aggregates. The oxygen content is located on the surface of the aggregates as C_xO_y complexes.

Table 2.1 Chemical composition of carbon blacks

Type	Carbon/ %	Hydrogen/ %	Oxygen/ %	Sulfur/ %	Nitrogen/ %	Ash/ %	Volatile/ %
Furnace rubber grade	97.3–99.3	0.20–0.80	0.20–1.50	0.20–1.20	0.05–0.30	0.10–1.00	0.60–1.50
Medium thermal	99.4	0.30–0.50	0.00–0.12	0.00–0.25	NA	0.20–0.38	–
Acetylene black	99.8	0.05–0.10	0.10–0.15	0.02–0.05	NA	0.00	<0.40

NA – not available.

Hydrocarbon materials produce carbon blacks; therefore, it is mostly hydrogen that saturates the dangling bonds at the edges of the basal planes of the graphitic layers. The graphitic layers are large, polycyclic aromatic ring systems.

Oxygen-containing complexes are by far the most important surface groups. The oxygen content of carbon blacks varies from 0.2% to 1.5% in mass for furnace blacks and 3% to 4% for channel blacks. Some special blacks used for pigment purposes contain larger quantities of oxygen than normal furnace blacks. These blacks are made by oxidation in a separate process step using nitric acid, ozone, air, or other oxidizing agents. They may contain from 2% to 12% oxygen. The oxygen-containing groups influence the physico-chemical properties, such as chemical reactivity, wettability, catalytic properties, electrical properties, and adsorbability. Oxidation improves dispersion and flow characteristics in pigment vehicle systems such as lithographic inks, paints, and enamels. In rubber-grade blacks, surface oxidation reduces pH and changes the kinetics of vulcanization, making the rubber compounds slower curing.

A convenient method for assessing the extent of surface oxidation is the measurement of volatile content. This standard method measures the weight loss of the evolved gases on heating up from 120°C to 950°C in an inert atmosphere. The composition of these gases consists of three principal components: hydrogen, carbon monoxide, and carbon dioxide. The volatile content of normal furnace blacks is under 1.5%, and the volatile content of oxidized special grades is 2% to 22%.

The origin of the volatile gases is the functional groups attached to carbon black, especially those on the surface. Surface oxides bound to the edges of the carbon layers are phenols, hydroquinones, quinones, neutral groups with one oxygen, carboxylic acids, lactones, and neutral groups containing two oxygens[1,2]. Figure 2.1 shows an idealized graphite-surface-layer plane with the various functional groups located at the periphery of the plane. Carbon blacks with few oxygen groups show basic surface properties and anion exchange behavior[3,4].

In addition to combined hydrogen and oxygen, carbon blacks may contain as much as 1.2% combined sulfur resulting from the sulfur content of the aromatic feedstock that contains thiophenes, mercaptans, and sulfides. The majority of the sulfur is not potentially reactive as it is inaccessibly bound in the interior of carbon black particles and does not contribute to sulfur cross-linking during the vulcanization of rubber compounds.

The nitrogen in carbon blacks is the residue of nitrogen heterocycles in the feedstocks. Thus, carbon blacks derived from coal tars have far more nitrogen than petroleum-derived blacks.

The ash content of furnace blacks is normally a few tenths of a percent but in some products may be as high as one percent. The chief source of ash is the water used to quench the hot black from the reactors during manufacture and for wet pelletizing the black.

2.3.1.3.1 Iodine Adsorptions

The adsorption of iodine on carbon black surfaces in an aqueous solution has been studied since the beginning of the last century[63]. In 1921, Carson and Sebrell[64] investigated correlations between iodine adsorption of carbon blacks and filled rubber properties. The iodine adsorption was performed using an iodine solution with small amounts of potassium iodide. Later, Smith, Thornhill, and Bray[65] reported that a good linear relation exists between iodine adsorption and surface area measured with nitrogen adsorption. This is for carbon blacks whose iodine adsorption is independent of the specific nature of the carbon surface, with the exception of the two blacks having a volatile content over 10%. However, when the volatile is removed by calcination, the iodine adsorption and surface areas are in much better agreement. From their data, 130 mg of iodine is associated with about 100 m^2 of surface area, corresponding to a covering power of 32 $Å^2$ per adsorbed iodine molecule and a diameter of 6.4 Å. The collision diameter of iodine from diffusion measurements[66] is found to be 4.6 Å, in sufficient agreement with the approximate value obtained from the present measurements to indicate the possibility of formation of a monolayer of adsorbed iodine.

Kendall's[67] systematic study on the adsorption of iodine from an aqueous solution demonstrated that the mechanism was more complex than what was previously assumed. Present in an aqueous solution of iodine-potassium iodide are potassium iodide, potassium triiodide, and iodine molecules because of the equilibrium:

$$KI + I_2 \rightleftharpoons KI_3$$

Hence, it is necessary to consider the identity of the adsorbed species. Kendall's blank experiments revealed that potassium iodide was not adsorbed. The isotherms of iodine adsorption for a number of carbon blacks are only independent of the amount of potassium iodide in the solution when the adsorption was expressed as a function of the free iodine concentration. The analysis of the iodine solution, before and after adsorption, demonstrated that the total concentration of iodide ($KI + KI_3$) decreased very little. These facts prove that only neutral iodine molecules are adsorbed.

The adsorption data of iodine with several carbon blacks satisfactorily corresponds to the Langmuir adsorption equation as:

$$m = m_1 K\left(c / c_0\right) / \left[1 + K\left(c / c_0\right)\right] \tag{2.68}$$

where m is solute adsorption in mg/g, m_1 the mass required to form a monolayer, c the concentration of the solute, c_0 the solubility of the adsorbate in the solvent, and K a constant. K is given approximately by:

$$K = e^{\Delta H / RT} \tag{2.69}$$

where ΔH is the net heat of adsorption.

Equation 2.68 shows that adsorption from the solution depends on the solubility of the adsorbate in addition to the concentration. Therefore, when measuring the iodine adsorption, the temperature and solvent have to be considered.

Watson and Parkinson[68] found the net heats of adsorption for furnace and graphitized carbon blacks were all about 2000 cal/mol, showing the reversible adsorption for these blacks to be physical in nature. The deviation from the Langmuir equation shown by channel blacks suggested that their surfaces might be heterogeneous. Based on fitting their data to different models, including the BET equation, they proposed a dual surface model for the iodine adsorption of channel black. The Langmuir equation for adsorption on a dual surface may be written as:

$$m = \frac{m_1^1 K_1 \left(\frac{c}{c_0}\right)}{1 + K_1 \left(\frac{c}{c_0}\right)} + \frac{m_2^1 K_2 \left(\frac{c}{c_0}\right)}{1 + K_2 \left(\frac{c}{c_0}\right)} \tag{2.70}$$

where the subscripts refer to the two types of surfaces which are considered to be of equal extent, so $m_1^1 = m_2^1$, although the heats of adsorption are different, corresponding to two different K values, i.e., the heat of adsorption for one part of surface is higher than that of the other.

For channel carbon blacks, whose volatile contents are all about 5% by weight, and whose specific surface areas cover the range from 227 m^2/g to 100 m^2/g, the volatile content per unit surface area increases with decreasing surface area. From the experimental data, the adsorption of iodine on unit surface also decreases. Obviously, the volatile content is responsible for the less active part of the surface. Thus, the progressive decrease in adsorption per unit area of these blacks is in agreement with the dual surface theory.

The logical extension of the theory to furnace blacks shows their Langmuir-type isotherms correspond to the case when the less active part of the surface becomes very small (volatile content < 1%). It was also confirmed that the graphitized carbon black (Graphon) corresponds to the case when volatile content (less active part of the surface) becomes zero. The adsorption in this case is even greater than that for furnace blacks. These findings are in line with the observation of Smith et al[65]. In their study, the carbon black with a higher volatile content shows a much lower iodine adsorption than that of its counterpart with a lower volatile. When the volatile is removed by calcination, the iodine adsorption increases drastically and follows the same line with the surface area as that obtained with the carbon black having a low volatile. In other words, the devolatilization makes the adsorption isotherm of iodine correspond to the Langmuir equation without changing the surface area.

For channel carbon blacks it is generally accepted that the volatile is mainly, if not only, determined by oxygen-containing groups. The process of devolatilization under high temperature in an inert atmosphere is related to the decomposition of oxygen groups. This suggests that the surface covered by oxygen groups has a lower surface activity for iodine adsorption. This can be further confirmed by the observations of Sweitzer, Venuto, and Estelow[69] who claimed that the decrease in adsorption of

iodine follows the oxidation of a thermal black. The decrease in adsorption can be well interpreted as a consequence of the low heat of adsorption of iodine by oxygen groups introduced onto the carbon black surface rather than a chemisorption taking place on the unoxidized black surface.

From the discussion above, for the carbon blacks with a low volatile content, there is a linear relationship between iodine number and NSA. Therefore, it is possible to take the iodine number as a measure of surface area.

Snow[70], after analyzing an enormous amount of data on the adsorption of iodine by various carbon blacks, developed a fast and simple laboratory method for determining the surface areas of basic carbon blacks, which is suitable for control work at furnace black and rubber factories, based on the observations that follow.

In addition to the surface characteristics, the amount of iodine adsorbed increases as total iodine available increases, and the rate of increasing decreases rapidly. For the high concentration of iodine in the solution at equilibrium, the rate of change is negligible. In this case, everything is constant except total iodine present ($a + L$ in Figure 2.19). The ratio of iodide ions to iodine and the concentrations of the solutions are very important for the iodine adsorption.

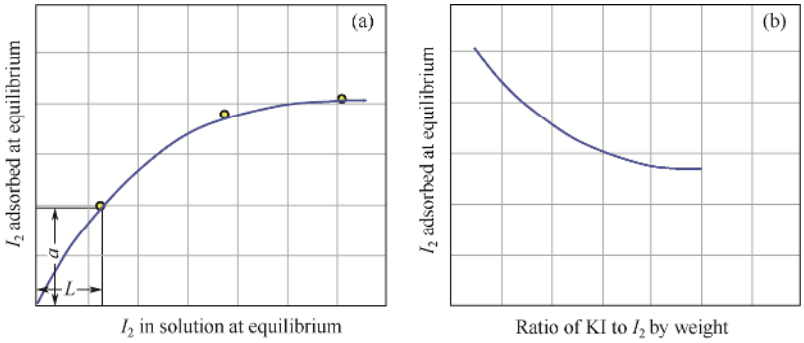

Figure 2.19 Schematic drawing of the iodine adsorbed as a function of the iodine concentration (a) and the ratio of iodide to iodine (b)[70]

Furthermore, the surface of the sample should not be so large as to adsorb more than about 90 mg to 100 mg of iodine from the solution[71]. Under the conditions specified by Snow, such as adsorbate concentration and the amount of carbon black sample used, the values of iodine numbers turn out to be numerically about the same as the values for surface areas in m^2/g that are measured by nitrogen adsorption for non-porous and non-oxidized furnace carbon blacks.

To demonstrate the utility of this test, iodine adsorptions were run on a variety of carbon blacks, and the iodine numbers obtained are plotted against the NSA in Figure 2.20[71]. The correlation is good for all definitely basic carbons. The presence of high levels of surface oxygen functionality also causes a severe reduction in the iodine number. The oxygen groups on the surface of the carbon black actually react with the

concentration of silanols[167–172], and the dependence is less with surface area of silica[173–175].

2.4.2.3 Inverse Gas Chromatograph

Although several methods can be used to measure the solid surface energy of fillers, inverse gas chromatography (IGC) is one of the most sensitive and convenient methods for measuring filler surface energy. In IGC, the filler to be characterized is used as the stationary phase and the solute injected is called a probe. When the probe is operated at infinite dilution, the net retention volume determines the adsorption energy of the probe on the filler surface, and hence the surface energy of the filler. On the other hand, if the surface is energetically heterogeneous, the values of parameters obtained from IGC measurement are mean values over the whole surface of the fillers. However, they are "energy-weighted", i.e., the high-energy sites play a very important role in determining the adsorption parameters measured[176]. Operating the probe at finite concentration allows the determination of the pressure dependence of the retention volume to generate the probes' adsorption isotherms on the filler surface. These isotherms yield the distribution of the probe chemicals' free energy of adsorption[176].

2.4.2.3.1 Principle of Measuring Filler Surface Energy with IGC

The thermodynamic parameters of the adsorption of the probe (solute) on the filler surface can be calculated from the retention data of the chromatogram and the filler surface energy can thus be determined[177–179].

In chromatography, the net retention volume is calculated from:

$$V_N = Dj\left(t_r - t_m\right)\left(1 - \frac{p_w}{p_0}\right)\frac{T_c}{T_f} \tag{2.175}$$

where t_r is the retention time of the given probe, t_m is the zero retention time measured with a nonadsorbing probe (for example methane), D is the uncorrected flow rate determined by timing a soap film, p_0 is the pressure at the flowmeter, p_w is the vapor pressure of the pure water at the flowmeter temperature, T_c is the column temperature, T_f is the retention flowmeter temperature, and j is the James-Martin factor for the correction of gas compressibility if there is a pressure difference between column inlet (p_{in}) and outlet (p_{out}). It is obtained by:

$$j = \frac{3}{2}\frac{\left(p_{in}/p_{out}\right)^2 - 1}{\left(p_{in}/p_{out}\right)^3 - 1} \tag{2.176}$$

On the other hand, the general retention volume of the adsorbate (probe) is related to the gradient $\mathrm{d}\Gamma/\mathrm{d}c$ of the partition isotherm as[180]:

$$V_N = A\left(1 - jY_0\right)\left(\frac{\partial \Gamma}{\partial c}\right)_p \tag{2.177}$$

where c is the concentration of the probe in the gas phase, Γ is the concentration of the probe on the solid surface, p is the equilibrium pressure, A is the total surface area of the solid adsorbent in the column, and Y_0 is the mole fraction of the probe in the gas phase at the column outlet. The term jY_0 in Eq. 2.177 is a correction factor for the sorption effect.

2.4.2.3.2 Adsorption at Infinite Dilution

Thermodynamic Parameters of Adsorption

At very low pressure, the sorption effect is so small that it can be neglected. Hence, Eq. 2.177 can be written as:

$$V_N = A\left(\frac{\partial \Gamma}{\partial c}\right)_{\mathrm{p}} \tag{2.178}$$

When adsorption takes place in the Henry's law region, i.e., at infinite dilution, one has:

$$\frac{V_N}{A} = \left(\frac{\partial \Gamma}{\partial c}\right)_{c\to 0} = \left(\frac{\pi}{p}\right)_{p\to 0} = K_{\mathrm{s}} \tag{2.179}$$

with $p = cRT$ and $\pi = \Gamma RT$, where π is the two-dimensional spreading pressure of the adsorbed probe on the filler surface, K_{s} is the the surface partition coefficient of the given probe between the adsorbed and gaseous state, R is the gas constant, and T is the temperature.

The variation of the standard free energy in isothermal transfer of one mole of probe from reference pressure p^0 to the adsorbed state at equilibrium with a pressure p of the gas phase is given by:

$$\Delta G^0 = -RT\ln\left(\frac{p^0}{p}\right) \tag{2.180}$$

When a surface with a spreading pressure π^0 is taken as the reference state of the surface, the change in standard free energy according to Eq. 2.180 for transferring one mole of probe from the gas phase at pressure p^0 to the solid surface at a spreading pressure π^0 is:

$$\Delta G^0 = -RT\ln\left(\frac{V_N p^0}{Sg\pi^0}\right) \tag{2.181}$$

Where S is the specific surface area of the solid, and g is the mass of the solid in the column.

If de Boer's surface state in which the average distance between adsorbed molecules is identical with the separation distance between molecules in the gas phase at 1 atm (1.013×10^5 Pa) and 0°C is adopted[181], π^0 is 3.38×10^{-4} N/m. Thus,

$$\Delta G^0 = -RT\ln\left(\frac{V_N}{Sg}2.99\times 10^8\right) \tag{2.182}$$

3 Effect of Fillers in Rubber

During the last several decades, a vast amount of information on elastomer reinforcement by carbon blacks and silica has been published. It is recognized that the main parameters of the filler which govern their reinforcing ability in rubber are the following:

- The size and distribution of primary particles, sometime referred to as "nodules", which are joined by fusion into aggregates arranged at random. The particle size and its distribution directly determine the surface area of the filler;
- The size, shape and their distribution of aggregates (aggregate complexity), i.e., the degree of irregularity of the filler units or the development of branches due to the aggregation of primary particles and the asymmetry of the aggregates. These parameters are generally termed filler "structure"; and
- Surface activity, which, in a chemical sense, is related to the reactivity of the chemical groups on the filler surface, and, in terms of physical chemistry, is referred to as adsorption capacity. This capacity is determined by filler surface energy, both its dispersive and specific components, and the energy distribution on the filler surface.

All these parameters play a role in rubber reinforcement through different mechanisms, such as hydrodynamic effect-strain amplification, interfacial interaction between filler and rubber, occlusion of the polymer in the internal voids of the aggregate, and the agglomeration of filler aggregates in the polymer matrix.

3.1 Hydrodynamic Effect–Strain Amplification

The presence of rigid particles has important geometric and dynamic consequences, since these particles will not be deformed under stress applied on the material[1]. As a result, the elastomeric matrix between the filler particles will experience larger strains than for the given overall stretches. This non-affine response is called the "strain amplification" of the elastomeric matrix in the presence of filler[2]. The deformation curves of filled samples thus enter on the steep branch of the stress-strain curves at lower nominal (overall) strains. Note that the stress maximum of Figure 3.1 lies a small distance away from the particle surface.

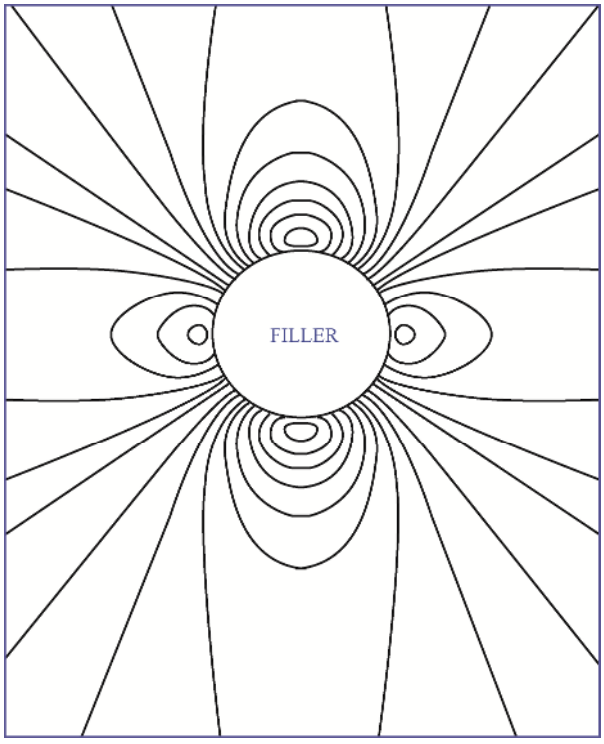

Figure 3.1 Binder stresses around filler particle (loading vertical)[3]

Strain amplification, while being the primary factor of the changes in mechanical responses which the filler causes, such as the accelerated rise in moduli, will be modified by the extent of strain transmission through the interfaces. If the deformation of the interface is small, the stress transmission is almost complete and the interface can be counted as part of the solid particle. If the interfacial bond strength is larger than the cavitation stress of the matrix, the failure process begins by the formation of hole away from the interface. If, on the other hand, the interface becomes substantially deformed, its own flow or compliance and its integrity must be considered. Whenever the interface ruptures or dewets, an entirely new situation is created in that now some parts of the matrix become more strained while others can relax so that the stress levels off and a substantial portion of the further work of deformation is invested in continuing dewetting processes and in the enlargement of the cavities.

It can be understood that, while stored (elastic) free energy is usually the mechanically valuable state function, it is also the potentially destructive one since the extra free energy accelerates scission and crack growth processes. Thus, apart from applications in which energy dissipation or abrasion resistance are the main concern, conversion of the stored free energy into heat by friction and relaxation processes, enhanced by filler, will in general improve the mechanical performance and life span of elastomers in most constructions or goods.

Due to the existence of the filler, hence the strain amplification, several factors influencing the rubber reinforcement need to be considered:

- the translation of the nominal external macroscopic stress field into the micro stress fields throughout the matrix (especially near the particle surfaces) taking into account filler loading, particle size, shape, and orientation distribution;
- the deformation stability of the interphase, establishing again stress field and distribution as well as the limits of the stresses that can be tolerated without dewetting or rupture;
- the course of the stress-strain response of the matrix as critical strains are approached and reached, i.e., taking into account degrees of energy dissipation, work-hardening, crystallization, and hysteresis;
- the extent and severity of dewetting, crack propagation, and molecular rupture processes in a given case have to be determined.

In all these aspects, the role played by the filler is related more or less to the strain amplification[1].

3.2 Interfacial Interaction between Filler and Polymer

One of the consequences of the incorporation of fillers into a polymer is the creation of an interface between a rigid solid phase and a soft solid phase. For rubber-grade fillers, whose surfaces exhibit very little porosity, the total area of the interface depends on both filler loading and the specific surface area of the filler. In a unit volume of compound, the interfacial area, ψ, is given by:

$$\psi = \phi \rho S \tag{3.1}$$

where ϕ is the volume fraction of the filler in the compound, and ρ and S are the density and specific surface area of the filler, respectively (Eq. 3.1).

Due to the interaction between rubber and filler, the polymer molecules can be adsorbed onto the filler surface either chemically or physically. This adsorption leads to two phenomena which are well documented, the formation of bound rubber and a rubber shell on the filler surface. Both are related to the restriction of the segmental movement of polymer molecules.

3.2.1 Bound Rubber

Bound rubber is defined as the rubber portion in an uncured compound which cannot be extracted by a good solvent due to the adsorption of the rubber molecules onto the

From Figure 6.9 and Figure 6.11, it can be observed that beyond $\lambda = 2$, i.e., 100% elongation, the modulus increases almost linearly with increasing strain. The slopes of the linear section are determined by the polymer-filler interaction. Since there is a direct relationship between the modulus and the stress at any given elongation, the slope of the linear section can be estimated from the tensile stresses (T) at two different elongations over the range of testing. Practically, the ratio of tensile stress at 300% elongation (T300) and at 100% elongation (T100), i.e., T300/T100 is a reasonable measure of the polymer-filler interaction.

■ 6.3 Strain-Energy Loss—Stress-Softening Effect

It is generally accepted that rubber reinforcement by fillers is closely related to the processes of energy dissipation during deformation. The importance of energy dissipation in the fracturing of vulcanizates, such as ultimate strength, tearing, cracking, abrasion, and fatigue, is also widely recognized. In practice, stress-softening effects are used as a quantitative measure of strain energy loss.

It has been known for many years that for vulcanizates either with or without fillers, deformation results in the softening of rubber and that the initial stress-strain curve determined during the first deformation is unique and cannot be retraced. This effect is generally called stress softening. Further repeated deformations will cause the vulcanizates gradually to approach a steady state with a constant or equilibrium stress-strain curve. Softening in this way occurs in both unfilled and filled vulcanizates, although the effect appears to be much more pronounced in vulcanizates containing high proportions of reinforcing fillers.

The stress-softening phenomenon was first observed by Bouasse and Carrière in 1903[63]. Holt[64] studied the effect of repeated stretching and the speed of stretching on the stress-strain properties of typical rubber compounds and their recovery after straining. He showed that the initial strain history has a remarkable effect upon the stress-strain performance of vulcanizates, and that rubber will not recover completely after straining. However, he did not offer a theoretical explanation for this phenomenon. Subsequently, this phenomenon was studied in more detail by Mullins[65,66], and has been termed the “Mullins effect”. He showed that while the softening of filler reinforced vulcanizates mainly occurred during the first cyclic stretch, after a few stretching cycles a steady state will be reached. The performance of stress-strain is relatively unaffected by previous stretching as long as the stretch is higher than the maximum stretch applied.

Typical stress softening can be seen in Figure 6.12 for NR gum vulcanizate and vulcanizates filled with different loadings of carbon black HAF (N330). The three vulcanizates were stressed initially to the same load on a tensile tester at the same strain rate and at room temperature. Also shown on the figure are the first retraction

(curves 2) and the second complete stressing cycles (curves 3 and 4) for extensions up to the same strain as the initial strain.

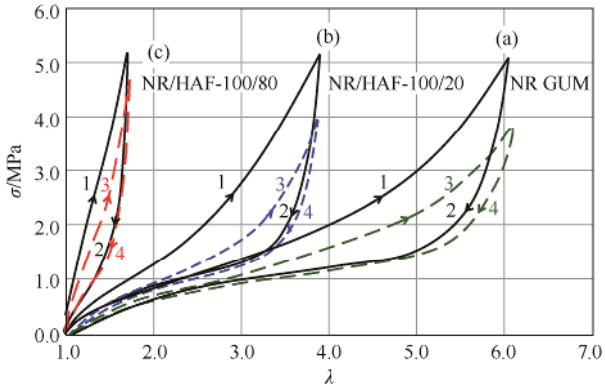

Figure 6.12 Stress (referred to original cross-section) as a function of strain for (a) gum vulcanizate, (b) vulcanizate containing 20 phr N330, and (c) vulcanizate containing 80 phr N330; (1) initial stressing curve; (2) first retraction curve; (3) second stressing curve; (4) second retraction curve[67]

The stress softening measured with the second mode of tensile tests is shown in Figure 6.13 for vulcanizates of NR gum and NR filled with 60 phr carbon black N330. When the stress-strain curves of the vulcanizates are increased to the same stress level, the shapes of stress-softening curves between the first, second, and third extension cycles are quite similar.

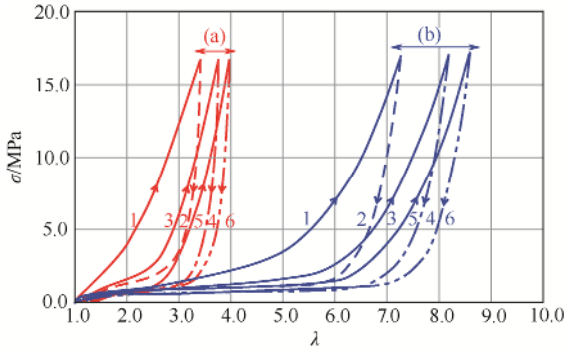

Figure 6.13 Stress-strain curves for (a) NR vulcanizate filled with 60 phr N330 carbon black and (b) NR gum vulcanizate additional extensions[68]

Another stress-softening tensile test is performed that is similar to how new samples of gum or filled vulcanizates are stretched to a given elongation and then retracted. After the first stress-strain cycle, the subsequent extension cycle is performed in a way that each succeeding stress-strain cycle is stressed to a higher level in incremental steps. The results are shown in Figure 6.14, in which the stress-strain curves of fresh samples

reduced by doping silica in the carbon phase. Consequently, there would be less hydrogen bonding, the main cause of the high filler-filler interaction between silica aggregates, between silica domains on neighboring aggregates since their average interaggregate distance would be greater. In addition, from the point of view of flocculation kinetics, the higher surface activity of the carbon phase of CSDPF, which leads to higher bound rubber[18], may contribute to less developed filler agglomeration.

The filler agglomeration of CSDPF can be further depressed by surface modification with coupling agent TESPT as shown by the Payne effect and equivalent filler volume. This is primarily due to the reduction of surface energies, both dispersive and polar components. The higher bound rubber content of the MCSDPF *vs.* its unmodified counterpart (45% *vs.* 32%) may also be a reason as the flocculation rate of the filler aggregates may be significantly reduced during vulcanization.

7.2.2 Strain Amplitude Dependence of Viscous Modulus of Filled Rubber

Fillers are known to cause a considerable increase not only in G', as discussed above, but also in G''. Since G'' is representative of the viscous component of the modulus, all processes of energy dissipation will affect G''. It can therefore be argued that interaggregate interaction must be involved to a considerable extent in energy loss, which would be highly dependent on strain amplitude, filler concentration, and filler properties.

Carbon Black

The strain dependence of viscous modulus for vulcanizates having different loadings of N234 are shown in Figure 7.8 for the results obtained at both 70°C and 0°C [4]. Evidently, the incorporation of carbon black in rubber will substantially increase the viscous modulus of the material regardless of the strain amplitude. As observed with G', this effect is also augmented exponentially with filler loading and is partially attributed to the hydrodynamic effect, as the addition of unstrained (or solid) particles in the polymer matrix would result in a high viscosity compound. It is also evident that in contrast to G' of filled rubber which decreases monotonically with increasing strain, G'' shows maximum values at moderate strain amplitudes (2%−5% and 3%−6% DSA for 70°C and 0°C, respectively, for these particular compounds and test conditions). After passing through a maximum, the G'' decreases rapidly with further increase in strain amplitude. Such behavior of the strain dependence of filled rubber cannot be explained only by the hydrodynamic effect since the G'' values of the gum compound, while being lower, do not show a significant strain dependence over a large practical range of strain amplitudes.

Payne[19], in his investigation of different polymers and carbon blacks at different loadings, found that G''_{max} is linearly related to $(G'_0 - G'_\infty)$, i.e., the maximum change in elastic modulus with increasing strain amplitude, and can be expressed as:

$$G''_{\max} = 0.17\left(G'_0 - G'_\infty\right) \tag{7.15}$$

where G'_0 and G'_∞ are the leveling values of G' at low and high amplitudes, respectively.

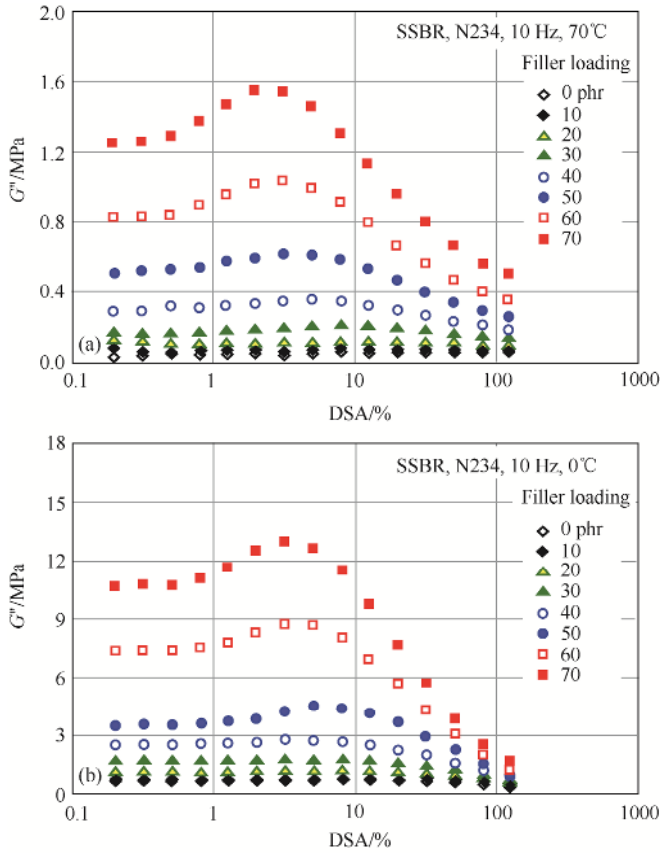

Figure 7.8 Strain dependence of G'' at 70 and 0°C and 10 Hz for SSBR compounds with different loadings of carbon black N234[4]

Several authors[20–24] later investigated different polymers and polymer blends filled with various carbon blacks and arrived at similar equations with different slopes and intercepts. Payne[19] believed that this type of energy loss was related to the breakdown and reformation of the filler agglomerate. At small amplitude, the disruption of the agglomerate is insignificant. G'' is therefore low, but increases rapidly at higher amplitudes where breakdown and reformation of the agglomerates is significant. High amplitudes will largely destroy the agglomerates, so that less energy is required for dynamic oscillation, thus leading to a reduction in G''. This suggests that internal friction is the dominant mechanism of energy dissipation during dynamic deformation. In a systematic study dealing with the effect of carbon blacks on rubber hysteresis,

Ulmer et al.[25] concluded that the formation of three-dimensional carbon black-rubber agglomerates is one of the factors affecting E''.

Based on the assumption of the breakdown and reformation of secondary structure, Kraus[26] derived the following equations for viscous modulus E'':

$$E'' = E''_{\infty} + \frac{C\varepsilon_0^m \left(E'_0 - E'_{\infty}\right)}{1 + \left(\varepsilon_0 / \varepsilon_c\right)^{2m}} \tag{7.16}$$

and

$$E'' = E''_{\infty} + C'\varepsilon_0^m \left(E'_0 - E'_{\infty}\right) \tag{7.17}$$

where m, C, and C' are constants; E''_{∞} is the E'' after total destruction of the filler agglomerates; ε_0 is the strain amplitude; and ε_c is the characteristic strain given by:

$$\varepsilon_c = \left(\frac{k_m}{k_b}\right)^{0.5m} \tag{7.18}$$

in which k_b is the rate constant of breakage of interaggregate contacts, and k_m is the rate constant of reagglomeration. It is obvious that the loss modulus is not only dependent on $\left(E'_0 - E'_{\infty}\right)$ and E''_{∞}, but also on the rates of agglomerate breakdown and reformation, which are related to the strain amplitudes. The breakdown of filler agglomerates would increase with increasing strain amplitude, and the reformation of this structure would diminish more rapidly than its disruption. Once the strain amplitude is high enough that the filler agglomerate is destroyed to such an extent that it cannot be reconstructed in the time scale of dynamic strain (frequency), the effect of filler agglomerate on the G'' will disappear. Similarly, if the filler agglomerate is strong enough and the strain (or stress) is small enough so that the filler agglomerate is unable to be broken, the G'' would be determined mainly by the hydrodynamic effect of the filler so that the strain dependence would be eliminated (Figure 7.8). In this case, however, the effective volume fraction of the filler hence the absolute G'' would be higher due to the hydrodynamic effect.

Silica and CSDPF

At the same mass loading, silica gives higher G'' than carbon black, whereas lower values were obtained with CSDPF at 70°C. The TESPT-modification of CSDPF is able to further reduce the hysteresis of the vulcanizate (Figure 7.9). This is true at both high and low temperatures. Lower G'' suggests that for CSDPF, less filler agglomerates would be broken down and reformed during dynamic strain.

At 0°C, silica gives much lower viscous modulus than carbon black does, which is the opposite of what happens at higher temperature. On the other hand, over the whole range of strain applied, the G'' of silica compound is almost the same as the value of CSDPF compound. This may be caused by two reasons. One is related to the energy

silica vulcanizates after stress softening during the first few cycles of compression under static load should lead to high dynamic strain and, hence, to considerable heat generation. Moreover, while tan δ represents the hysteresis of one cycle of deformation at a constant temperature (even when measured after several cycles of deformation), ΔT constitutes a cumulative value for heat generation. It is determined not only by the hysteresis of the sample, but also by the heat exchange with the environment. The temperature of the sample at equilibrium could, therefore, be affected by the thermal conductivity of the filled vulcanizates.

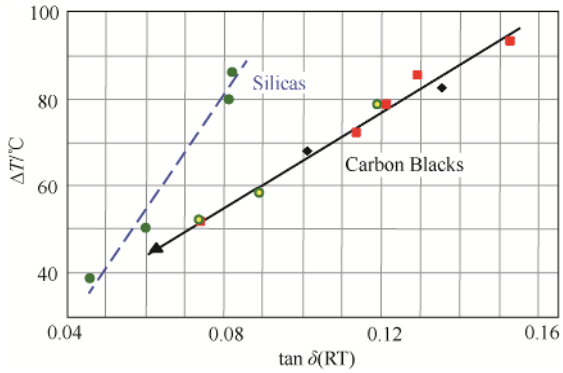

Figure 7.44 Heat build-up *vs.* tan δ at room temperature for silica and carbon black filled NR[68]

■ 7.6 Resilience

Resilience, or the rebound in single pendulum tests using a hemispherical striker or falling ball, also represents a measure of the hysteresis under conditions of constant energy input, although the deformation is complex, involving extension, compression, and shear. Gehman[69] used a pendulum test and showed that tan δ was directly proportional to the logarithm of the fractional rebound, R:

$$\tan \delta = -\ln R / \pi \tag{7.25}$$

Other authors[70–72] also observed a good correlation between resilience and tan δ. It is therefore not surprising that the correlation between tan δ and the interaggregate distance, δ_{aa}, can also be applied to resilience[16]. As illustrated in Figure 7.45, a single curve may be used to represent the results of Firestone Ball Rebound as a function of δ_{aa} for SBR vulcanizates filled with the whole range of rubber-grade carbon blacks at various degrees of loading[16]. The ball rebound increases rapidly in the low δ_{aa} region and reaches a maximum value which corresponds to that of the gum. The change in resilience with interaggregate distance follows the same mechanism which was discussed in the case of tan δ.

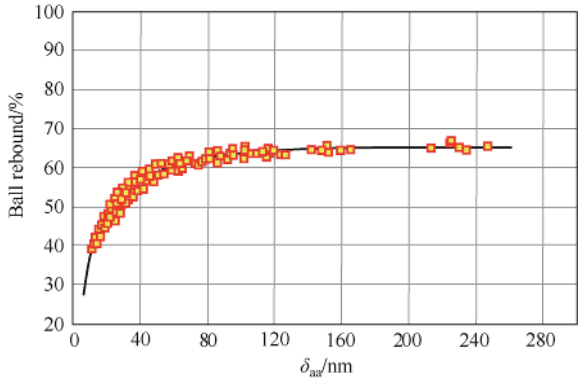

Figure 7.45 Firestone ball rebound as a function of interaggregate distance[16]

Wolff and Wang[67] have found that the curves of ball rebound *vs.* filler loading of SBR vulcanizates filled with a series of different furnace carbon blacks can be superposed to one single master curve by introducing a shift factor, f, taking one-carbon-black filled polymer as a reference. The master curve for ball rebound of SBR vulcanizates is shown in Figure 7.46.

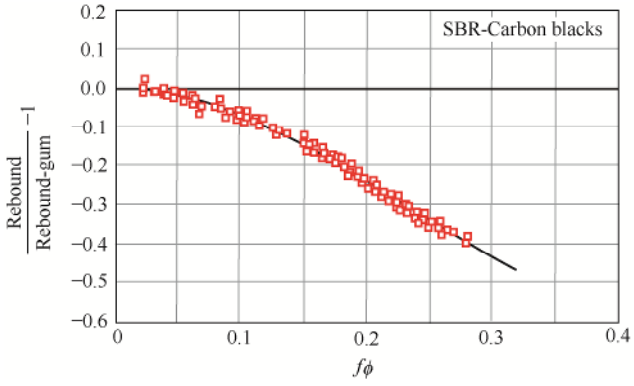

Figure 7.46 Master curve for ball rebound for SBR vulcanizates[67]

The change in f with CTAB and compressed DBP for ball rebound is shown in Figure 7.47. This shift factor is mainly dependent on surface area; the effect of structure appears to be insignificant. Instead of a structure-loading equivalence, a surface area-loading equivalence seems to exist in this case. Furthermore, the shift factor for ball rebound is linearly related to the value of A (Figure 7.48), probably for the same reason. A is defined as[73]:

$$A = (R_0 - R) \times \frac{m_P}{m_F} \tag{7.26}$$

where R and R_0 are the ball rebound values of filled and unfilled vulcanizates, and m_F and m_P are the mass of the filler and the polymer, respectively (Eq. 7.26). It was found that the constant A, i.e., the slope of the plot of $(R_0 - R)$ versus m_F/m_P, is independent of the crosslink density of the vulcanizates, of filler loading, and of filler structure, but that it depended on the type of elastomer and on carbon black surface area. This parameter is characteristic for each carbon black and was defined as a measure of the in-rubber surface area of furnace carbon blacks. The effective volume loading for ball rebound is thus associated with the interfacial area in filled vulcanizates.

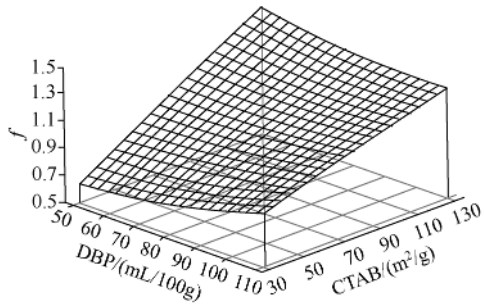

Figure 7.47 f for ball rebound as a function of CTAB surface area and DBP (24M4) for SBR vulcanizates[67]

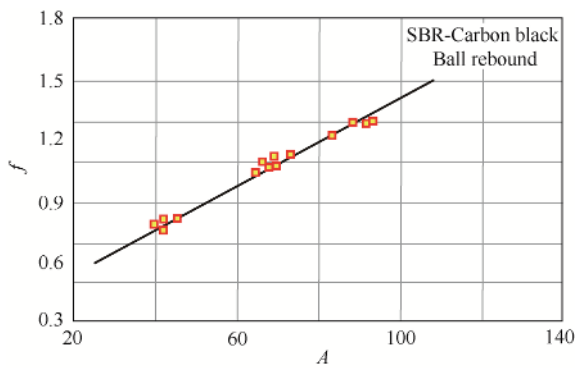

Figure 7.48 Shift factor f for ball rebound as a function of A for SBR vulcanizates[67]

References

[1] Ferry J D. Viscoelastic Properties of Polymers. 3rd Edition. Wiley, 1980, chapter 1.
[2] Williams M L. The Temperature Dependence of Mechanical and Electrical Relaxations in Polymers. *J. Phys. Chem.*, 1955, 59: 95.
[3] Williams M L, Landel R F, Ferry J D. The Temperature Dependence of Relaxation Mechanisms in Amorphous Polymers and Other Glass-forming Liquids. *J. Am. Chem. Soc.*, 1955, 77: 3701.

8 Rubber Reinforcement Related to Tire Performance

Continuous improvement of tire quality in the areas of better fuel economy, improved safety, and increased durability requires development of new tire compounds, particularly tread compounds. These requirements can only be met by improvements in rolling resistance, skid resistance, especially in wet conditions, and wear resistance, which are closely related to hysteresis, wet friction behavior, and abrasion of tread compounds. In these regards, it has been recognized that the filler takes an equal place alongside the polymer as the underlying determinant of the tire performance. In fact, the filler is no longer a "filler" in the sense of increasing the volume and reducing cost of the compounds. The filler is also not a "reinforcing agent" in the sense of increasing modulus and improving tensile strength of the compounds. The filler is actually a functional material or component in the tire compound to control tire functionality. In this chapter, the roles played by filler parameters, such as types, loading, morphology, and surface characteristics, in the rolling resistance, wet skid resistance and wear resistance of tires will be discussed.

■ 8.1 Rolling Resistance

8.1.1 Mechanisms of Rolling Resistance–Relationship between Rolling Resistance and Hysteresis

The energy loss in rubber products during dynamic strain is of great importance for automotive tires, where it affects the service performance with regard to rolling resistance, traction, and skid resistance.

In fact, with regard to tire applications, it has been well established that repeated straining of the compound due to rotation and braking can be approximated as a

process of constant energy input involving different temperatures and frequencies[1−3]. With respect to the tire tread, its deformation can be, as cited by Medalia[4], resolved "approximately into a constant strain (bending) and constant stress (compression) condition; and since the geometric mean of the hysteresis under these two conditions is approximately proportional to tan δ, tire tread hysteresis is as a first approximation, proportional to "tan δ".

Rolling resistance is related to the movement of the whole tire corresponding to deformation at a frequency of 10−100 Hz and a temperature of 50−80°C. In the case of skid or wet grip, the stress is generated by resistance from the road surface and movement of the rubber at the surface, or near the surface of the tire tread. The frequency of this movement depends on the roughness of the road surface but should be very high, probably around 10^4 Hz to 10^7 Hz at room temperature[2,3]. It is therefore obvious that any change in dynamic hysteresis of the compounds at different frequency and temperature will alter the performance of the tire. Since certain tire properties involve frequencies which are too high to be measured, these frequencies are reduced to a measurable level (e.g., 1 Hz or 10 Hz) at lower temperatures by applying the Time-Temperature Superposition Principle (or WLF Temperature-Frequency Conversion) even though in the case of filled vulcanizates the shift factors for building the elastic modulus master curve are not exactly the same as those for the master curve of viscous modulus[5], hence of tan δ. However, the master curves for each property can be constructed experimentally according to the WLF Temperature-Frequency principle.

The reduced temperature for different tire properties at 10 Hz (Figure 8.1) has been used as the criterion for polymer[6] and filler[7] development for tire compounds. From the viscoelastic property point of view, an ideal material which is able to meet the requirement of a high-performance tire should give a low tan δ value at a temperature of 50−80°C in order to reduce rolling resistance and save energy. The ideal material should also demonstrate high hysteresis at lower temperature, for example, from −20°C to 0°C, in order to obtain high skid resistance and wet grip.

The topic of this section is rolling resistance that is determined by the tan δ at high temperature. Since the filler factors controlling the tan δ at high temperature are also related to the tan δ at low temperature, which is a key compound property for wet skid resistance, both loss tangents will be discussed in this section. However, the factors involved in skid resistance are recognized to be more complex than a single compound property and will be discussed in Section 8.2.

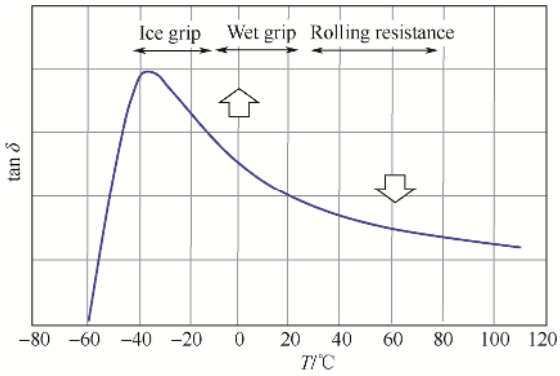

Figure 8.1 Reduced temperatures at 10 Hz for different tire performances

8.1.2 Effect of Filler on Temperature Dependence of Dynamic Properties

8.1.2.1 Effect of Filler Loading

The effects of filler loading on the temperature dependence of dynamic properties are presented in Section 7.2.5 (see Figures 7.15−7.17) for carbon black N234 filled compounds[8]. It can be seen that with regard to the tire application, simply by reducing the filler loading, the dynamic properties can be easily satisfied, at least from the point of view of tan δ. In fact, while the gum rubber gives lower hysteresis at relatively high temperature, which represents rolling resistance, its friction coefficient would be the best as tan δ is the highest at lower temperature[9]. However, in tire compounding, enough filler must be incorporated to meet the requirements for stiffness, wear resistance, handling, tearing resistance, and strength of the vulcanizate. These properties influence not only the service life of the tire but also driving safety, as hysteresis properties may not be the only factor to govern the skid resistance and cornering performance.

The results in Figure 7.17 suggested that the loading effects at different temperature regions should be governed by different mechanisms. As discussed in Section 7.2.5, among others, for a given polymer system, agglomeration of filler aggregates is the dominant factor in the determination of the hysteresis of filled vulcanizates. Due to filler agglomeration, the effective volume fraction of the filler will increase because of the rubber trapped in the agglomerates, which loses its identity as rubber, and behaves like filler. At high temperature, where rubber is in its rubbery state, the hysteresis is low under dynamic strain as the breakdown and reformation of the agglomerates would cause the energy dissipation, resulting in increased hysteresis. However, at low temperature where the main portion of the filled vulcanizate for energy dissipation is polymer matrix and the filler agglomerates may not be easily broken down, tan δ would be significantly attenuated by filler agglomeration due to the reduction of the effective volume of the polymer. Also in the transition zone, once the filler network

can be broken down and reformed under a cyclic strain, the hysteresis can be substantially augmented through release of polymer to participate in energy dissipation and change in the agglomerate structure. Therefore, over a limited range of strain amplitudes, filler agglomeration plays a dominant role in improving the temperature dependence of tan δ.

8.1.2.2 Effect of Filler Morphology

Besides loading and surface characteristics of filler, the main filler parameters influencing filler agglomeration, hence the hysteresis related to tire performance, are filler morphology, namely, surface area or particle size and structure. The role of these two parameters may involve different mechanisms and therefore will be discussed separately.

8.1.2.2.1 Effect of Surface Area

It has been widely documented that with increasing surface area of carbon blacks at constant loading, Payne effect increases[10–12]. The increase in Payne effect suggests a strong tendency for agglomeration of small particle (aggregate) carbon black in the polymer matrix. It is also widely reported that the dynamic hysteresis, characterized by tan δ, increases with filler surface area[1,10,13–15]. This is generally true at temperatures where the polymer is in its rubbery state as shown in Figure 8.2. Specifically, the DSA dependence of tan δ is compared using solution SBR (Duradene 715) vulcanizates filled with 50 phr of a series of carbon blacks having different surface areas (see Table 8.1). However, at low temperatures, where rubber falls in the transition zone, tan δ increases with decreasing carbon black surface area over a large range of strain amplitudes (see Figure 8.3). Such an observation can also be seen from temperature sweep data at a moderate-strain amplitude (5% DSA) and 10 Hz. As shown in Figure 8.4, there is a critical point around 0°C beyond which tan δ is higher for small-particle blacks and below which tan δ increases with decreasing surface area. This is even much clearer when the data are plotted at different temperatures on a linear scale as a function of CTAB surface area (Figure 8.5).

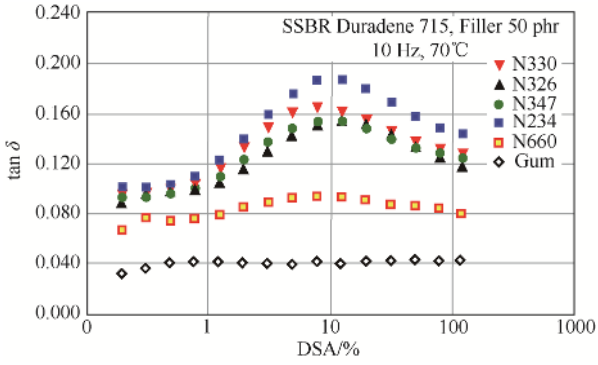

Figure 8.2 Strain dependence of tan δ at 70°C and 10 Hz for vulcanizates filled with a variety of carbon blacks with different morphologies

Index

F

G

H

I

J

L

M

S